Open Access

Catalytic Behaviour of $MnZrO_x$ System for Heterogenous Biodiesel Production

C. Cannilla[1], G. Bonura[1], F. Arena[1,2] and F. Frusteri[1,*]

[1]*CNR-ITAE "Nicola Giordano", Salita S. Lucia sopra Contesse, 5 - 98126 Messina, Italy*

[2]*Dip. To Chim. Ind. Ing. Mater. Università di Messina, Viale F. Stagno D'Alcontres, 31 - 98166 Messina, Italy*

Abstract: Manganese/zirconium mixed oxides catalysts ($MnZrO_x$), characterized by high Mn loading (up to 50%), along with high specific surface area, have been investigated in the transesterification reaction of sunflower oil. Catalysts were found to be very active by operating at low catalyst/oil ratio (1 wt.%). The high activity was justified on the basis of both the marked basic character of such systems and their high porosity that favours the accessibility of active sites. The calcination at high temperature (600°C) negatively reflects on the catalyst textural properties, drastically reducing the total surface area and consequently the catalytic activity. On the other side, such thermal treatment allows the obtainment of a macroporous structure with enhanced active sites accessibility, making $Mn_{0.8}Zr_{0.2\_600}$ the most active sample per unit of surface area.

Keywords: $MnZrO_x$ catalysts, redox-precipitation method, biodiesel, transesterification.

1. INTRODUCTION

Biodiesel is a sustainable fuel that consists of fatty acid alkyl esters (C_{14}-C_{22}) derived from either the transesterification of triglycerides (TGs) or the esterification of free fatty acids (FFAs) with methanol or ethanol [1, 2]. Biodiesel has become attractive because of its use as additive in diesel fuel which positively reflects in the reduction of pollutants in the exhaust, with evident benefits in the containment of CO_2 emissions in atmosphere [3].

The transesterification reaction can be chemically and enzymatically catalyzed or it can be carried out in methanol supercritical phase under drastic reaction conditions [4, 5]. Although the transesterification reaction can be catalyzed either by basic or acidic systems, the conventional homogeneous process involves the use of alkaline catalysts (e.g., NaOH, KOH and $NaOCH_3$), which allow to obtain high product yield under relatively mild reaction conditions [6]. Nevertheless, in the last decades, to overcome the typical limitations associated to the homogeneous catalysis, as well as the difficulty to use raw materials containing more than 0.5 wt.% of Free Fatty Acids (FFAs), to limit the soap and gel formation, along with the need of refining and washing steps, several catalysts have been proposed to perform the transesterification reaction in a heterogeneous liquid phase system [5]. In fact, by using a solid catalyst, several advantages should be achieved like: *a)* high quality and purity of esters and glycerine produced; *b)* easy separation and purification of products; *c)* no catalyst neutralization and washing; *d)* catalyst reuse; *e)* no soaps formation; *f)* no salt or aqueous waste streams; *g)* no consumption of chemicals; *h)* no corrosion problems; *i)* safety and low-cost continuous processes [7, 8].

Really, many solid catalysts, including alkali metal oxides [9], alkaline earth metal oxides [10], calcined hydrotalcites [11, 12], transition metal oxides, hydroxides, salts [13-15], metal zeolites [16], cation or anion exchanged resins [17, 18], heteropolyacids [19] and superacids [16] have been claimed as efficient systems for the transesterification of vegetable oils with methanol. Nevertheless, even if such systems seem to be interesting [9-16], most of them present low activity and stability mainly due to leaching phenomena occurring during reaction.

On this paper, taking into cosideration that MnO was already found to be active in transesterification reaction [20], a Mn-Zr based catalyst has been designed by exploiting the features of the redox-precipitation method already employed to prepare $MnCeO_x$ system [21]. In the attempt to optimize the catalytic formulation, CeO_2 was exchanged with ZrO_2 as carrier to take advantage also of its peculiar acid-base properties [22, 23]. Therefore, in the present work, preliminary results obtained by using a $MnZrO_x$ system in the transesterification of sunflower oil with methanol are reported. The relationships between the activity and surface properties of $MnZrO_x$ catalyst were discussed along with the influence of the calcination temperature on the catalytic behaviour.

2. EXPERIMENTAL

2.1. Chemicals

Commercial-grade sunflower oil (density, 0.85 g mL^{-1}) and methanol (MeOH) (HPLC-grade, 99.8%) were used. Pure GC standard chemicals, including fatty acid methyl-esters (ME) mix (methyl palmitate, methyl stearate, methyl oleate, methyl linoleate, methyl linolenate, methyl arachi-

*Address correspondence to this author at the CNR-ITAE "Nicola Giordano", Salita S. Lucia sopra Contesse, 5 - 98126 Messina, Italy: Tel: +39 090 624233; Fax: +39 090 624247;
E-mail: francesco.frusteri@itae.cnr.it

nate) and methyl heptadecanoate, were supplied by Sigma-Aldrich. The commercial sunflower oil contained saturated (≈10%), mono-unsaturated (≈27%) and poly-unsaturated (≈63%) esters. The oil had a low content of FFAs (0.07 wt.%) evaluated by standard titration method. Before titration, a certain amount of sample (≈10 g) was dissolved in diethyl ether (purity degree, 99.9 %) and ethanol mixture (purity degree, 99.9 %). Phenolphthalein indicator was used to determine pH change during neutralization reaction [24].

2.2. Catalysts Preparation

2.2.1. $MnZrO_x$ Systems

Two manganese-zirconia catalysts ($Mn_{0.x}Zr_{0.y}$), with a Mn/Zr atomic ratio equal to 1/1 and 4/1, were prepared *via* the redox-precipitation route [25]. An amount of $KMnO_4$, in a 10% stoichiometric excess, was dissolved in deionized water and titrated at 60°C, under vigorous stirring with a solution of Zr^{4+} and Mn^{2+} nitrates, at constant pH (8.0 ± 0.2) by addition of a 0.2 M KOH solution. After titration, the solid was digested for 30 min at 60°C and then filtered and repeatedly washed with hot distilled water. The solids obtained were dried at 100°C for 16 h and then calcined for 6 h in air at different temperatures: 300, 400 and 600°C. Calcined catalysts were kept in sealed sample holders in order to avoid exposure to air.

2.2.2. Manganese, Zirconium and Magnesium Oxides

A commercial “precipitated-activated” MnO_2 sample (Fluka products, >90%) has been selected as a “standard” sample. ZrO_2 was prepared by precipitation slowly adding a solution of KOH at 60°C under vigorous stirring, in a solution containing $ZrO(NO_3)_2$ at pH = 8.0 ± 0.2. After titration, the solid was digested for 6 h at 60°C, then filtered and repeatedly washed with hot distilled water. Then, the solid was dried at 110°C for 16 h and calcined for 6 h in air at 400°C.

A commercial MgO sample (MagChem 200-AD, SA_{BET}, 180 m^2g^{-1}) was also used as a reference sample.

2.3. Catalysts Characterization

2.3.1. X-Ray Fluorescence (XRF)

The analytical composition of the Mn-based catalyst was determined by XRF measurements, using a Bruker AXS–S4 Explorer Spectrometer. The concentration of elements was determined by the emission value of $K\alpha_1$ transitions of Mn (E=5.9 KeV) and Zr (E=15.8 KeV).

2.3.2. Surface Area (SA_{BET}), Pore Volume (PV) and Pore Size Distribution (PSD)

Surface area, pore volume and pore size distribution were determined from the nitrogen adsorption/desorption isotherms at -196°C, using a Carlo Erba (*Sorptomatic Instrument*) gas adsorption device. Before analysis, all samples were out-gassed at 120°C under vacuum for 2 h. The isotherms were elaborated according to the BET method for surface area calculation, with the *Horwarth–Kavazoe* and *Barrett-Joyner-Halenda* methods used for the evaluation of micropore (d<2nm) and mesopore (2<d<50 nm) distributions respectively.

2.3.3. X-Ray Diffraction (XRD)

XRD analysis of powdered samples was performed using a *Philips X-Pert* diffractometer equipped with a Ni β-filtered Cu-Kα radiation at 40 kV and 30 mA. Data were collected over a 2θ range of 20-85°, with a step size of 0.05° at a speed of 0.05° s^{-1}. Diffraction peaks identification was performed on the basis of the JCPDS database of reference compounds [26].

2.3.4. CO_2–Temperature Programmed Desorption (CO_2-TPD)

CO_2-TPD measurements in the range of 20-350°C were carried out using a linear quartz micro-reactor (d_{int}, 4 mm; l, 200 mm) loaded with ca. 50 mg of catalyst, using a heating rate of 20°C min^{-1}. After an *in situ* pre-treatment at 400°C (30 min) under a 10% O_2/He flow (25 STP ml min^{-1}), the catalyst was cooled down to room temperature, switched in the He carrier flow (30 STP mL min^{-1}) and saturated with CO_2 pulses (0.2 mL). After saturation, the sample was purged in the carrier flow until stabilization of the baseline. The desorption process was monitored and quantified by a TCD, preliminarily calibrated by the injection of pure CO_2 pulses.

2.3.5. Atomic Absorbance Spectrometry (AAS)

Atomic absorbance measurements were performed using an *Analyst 200, Perkin Elmer* analyzer. The concentration of manganese in biodiesel batches has been evaluated at λ=279.5 nm. Standard solution of manganese nitrate was used as a reference.

2.4. Catalyst Testing

Catalytic testing in the transesterification reaction of sunflower oil with methanol was carried out in a 300 mL stainless steel AISI 316 autoclave (*Parr Instruments*) equipped with a magnetic stirrer at 140°C by using a MeOH/oil molar ratio (R_{met}/oil) of 12 and a concentration of 0.2-1 wt.% of catalyst referred to the oil, according to the procedure elsewhere described [21]. At the end of the run, the reactor was cooled down to room temperature by putting it into an ice-bath, thus allowing all the gas-phase components to be condensed. The catalyst was separated by centrifugation and filtration, whereas the reaction mixture was recovered after the evaporation of unreacted methanol and the separation from glycerol by centrifugation. Activity measurements were also carried out on “used” catalyst after washing in methanol and drying to “clean” the active sites.

2.5. Analysis of Reaction Mixture

The reaction mixture was analyzed *off-line* by an Agilent 7890A GC, equipped with a *HP Innowax* capillary column (l, 30 m; i.d., 0.32 μm; film thickness, 0.25 μm), suitable for analysis of C_{14}-C_{24} methyl esters and a flame ionization detector (FID), according to the EN 14103 method [27]. Methyl palmitate, methyl stearate, methyl oleate, methyl linoleate, methyl linolenate and methyl arachidate were used as chemical GC standards for analysis calibration [21]. The biodiesel analysis was carried out dissolving 50 mg of the sample into 1 mL of methyl heptadecanoate solution, used as an internal standard, each conversion-selectivity data set being calculated from the average of three independent measurements with an accuracy of ±1%. The analysis of the

Table 1. Analytical Composition and Textural Properties of the $MnZrO_x$ Catalysts and "Pure" Oxides

Catalyst	Analytical Composition (wt.%)			$(Mn/Zr)_{at}$	SA_{BET} $(m^2 \cdot g^{-1})$	PV $(cm^3 \cdot g^{-1})$	APD (Å)
	K_2O	MnO_2	ZrO_2				
$Mn_{0.5}Zr_{0.5}$	4.8	38	57.2	1.1	201	0.79	170
$Mn_{0.8}Zr_{0.2}$	9.7	63	27.3	4.0	159	0.90	270
MnO_2	-	100	-	-	92	0.20	74
ZrO_2	-	-	100	-	125	0.16	28

Table 2. Effect of the Calcination Temperature (T_C) on Surface Area (SA_{BET}), Pore Volume (PV) and Average Pore Diameter (APD) of the $Mn_{0.8}Zr_{0.2}$ Catalyst

T_C (°C)	SA_{BET} $(m^2 \cdot g^{-1})$	PV $(cm^3 \cdot g^{-1})$	APD (Å)
-[a]	240	0.86	274
300	206	0.83	161
400	159	0.90	270
600	61	0.54	402

[a] dried sample

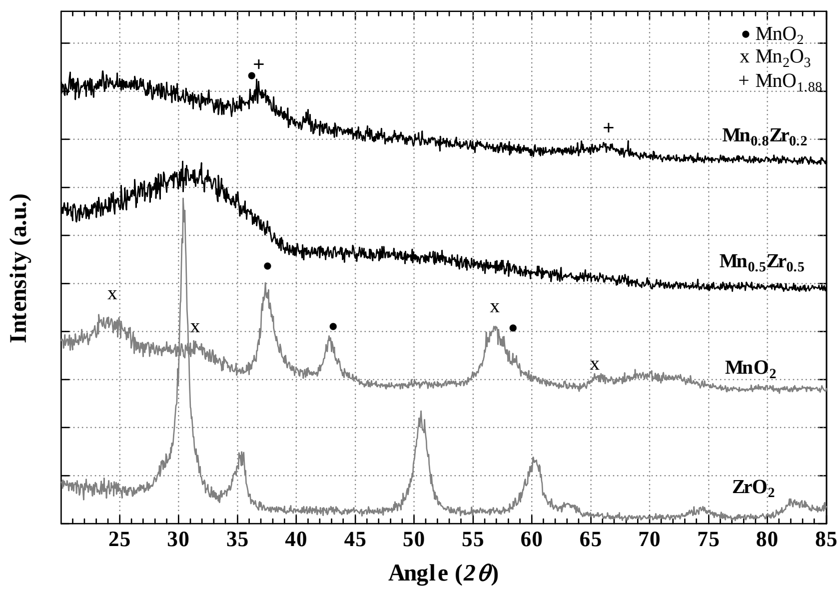

Fig. (1). XRD patterns of the investigated systems.

reaction mixture has not been performed at different reaction times to avoid the risk to spill out from the reactor a not representative sample, owing to the significant difference in density of the reaction compounds.

After reaction, at every purification step of the FAME mixture (centrifugation, catalyst filtration, methanol distillation, recover of glycerol), GC analysis allowed to exclude the occurrence of any incipient reaction altering the mixture composition, due to possible catalyst leaching phenomena.

3. RESULTS AND DISCUSSION

The main physico-chemical properties of MnO_2, ZrO_2 and $MnZrO_x$ catalysts, calcined in air at 400°C, are reported in Table **1**. ZrO_2 is characterized by a surface area higher than MnO_2 (125 and 92 m^2 g^{-1} respectively), although MnO_2 possesses a much higher APD (74 *vs*. 28 Å). $MnZrO_x$ systems exhibit higher surface area in respect to the single oxides (MnO_2 and ZrO_2), but, as the loading of Mn increases, the SA_{BET} decreases (from 201 up to 159 m^2 g^{-1}), with a PV growing from 0.79 to 0.90 cm^3 g^{-1} accounting for a broadening of the APD from 170 to 270 Å.

The influence of calcination temperature (T_C) on surface area, pore volume and average pore diameter of $MnZrO_x$ systems is presented in Table **2**. By increasing the calcination temperature, a progressive SA_{BET} decay from 240 (*dried* sample) to 61 m^2 g^{-1} (T_C, 600°C) is observable. The significant change in PV observed after calcination at temperature higher than 400°C (0.90 *vs*. 0.54 cm^3 g^{-1}) signals the occurrence of a structural rearrangement of catalyst towards the formation of a porous system consisting of fewer but larger pores (APD, 402 Å).

Fig. (**1**) shows the XRD patterns of calcined $MnZrO_x$ catalysts (T_C, 400°C) along with the "bulk" oxide samples, while, in Fig. (**2**) a comparison among the diffraction pat-

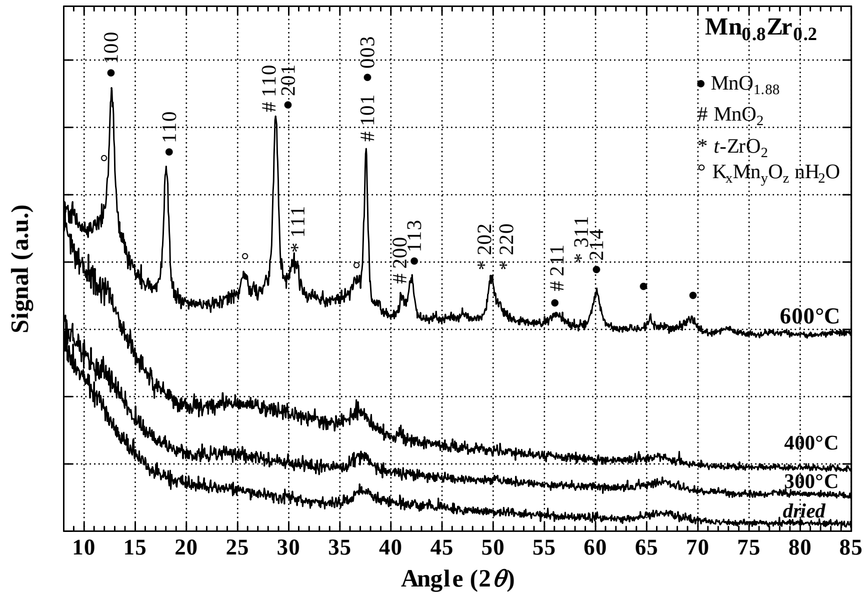

Fig. (2). Effect of the calcination temperature on the XRD pattern of $Mn_{0.8}Zr_{0.2}$ sample.

Table 3. Basic Properties of the MnZrOx Systems Along with Reference "Bare" Oxides

Catalyst	Basicity		Basic Strength						MSBS* (%)
	Specific ($\mu mol_{CO2} \cdot g_{cat}^{-1}$)	Intrinsic ($\mu mol_{CO2} \cdot m^{-2}$)	Peak 1 Weak		Peak 2 Medium		Peak 3 Strong		
			TM_1 °C	$\mu mol_{CO2} m^{-2}$	TM_2 °C	$\mu mol_{CO2} m^{-2}$	TM_3 °C	$\mu mol_{CO2} m^{-2}$	
$Mn_{0.5}Zr_{0.5\_400}$	417	2.1	101	0.72	191	0.67	301	0.57	63
$Mn_{0.8}Zr_{0.2\_300}$	591	2.8	106	0.80	215	1.17	304	0.88	72
$Mn_{0.8}Zr_{0.2\_400}$	300	1.9	110	0.60	205	0.61	313	0.66	68
$Mn_{0.8}Zr_{0.2\_600}$	424	6.9	136	4.19	221	0.95	306	1.79	40
MnO_2	271	2.9	121	0.70	228	0.44	292	1.80	76
ZrO_2	310	2.5	114	1.27	220	0.61	300	0.58	50
MgO	363	2.0	-						

*MSBS = Medium and Strong Basic Sites Contribution.

terns of the $Mn_{0.8}Zr_{0.2}$ sample calcined at different temperature is shown. The profile of the ZrO_2 discloses the presence of a mixture of cubic [JCPDS, 270997] and tetragonal zirconia [JCPDS, 170923], while the XRD spectrum of MnO_2 appears to be characterized by both Mn_2O_3 and MnO_2 species with an intense signals at 37.5° and 42° diagnostic of the presence of Mn^{IV} oxide [JCPDS, 24-735]. $Mn_{0.5}Zr_{0.5}$ exhibits a broad peak at 20-40° indicative of a typical amorphous structure. By increasing the Mn loading (see $Mn_{0.8}Zr_{0.2}$ profile), the XRD pattern slightly changes showing two low intense signals at around 37° and 66°: these crystalline components are mainly related to the presence of very small crystallites of manganese oxide in different oxidation states [21], as further confirmed by XRD data of the $Mn_{0.8}Zr_{0.2}$ sample calcined at 600°C (see Fig. **2**). In such a case, a higher calcination temperature promotes a significant structural rearrangement with segregation of MnO_2 crystallites. In particular, resolved peaks at 12.7, 18.1, 28.5, 37.4, 42.0, 56.3, 60.1 (•) and 25.4, 28.3, 37.2, 40.8, 42, 56.4 (#) respectively point out the presence of $MnO_{1.88}$ [JCPDS, 5-673] and MnO_2 (in form of pyrolusite) [JCPDS, 24-735] phases in the sample. It is noteworthy to observe that untreated $Mn_{0.8}Zr_{0.2}$ sample shows the same diffraction pattern of the catalyst calcined at 300 and 400°C, thus suggesting that the $MnZrO_x$ systems are characterized by an uniform molecular-like dispersion of Mn ions across the zirconia matrix. On the whole, the amorphous structure mirrors the intimate interaction of MnO_x and ZrO_2 species occurring during the preparation step which allows the formation of nanosized $MnZrO_x$ oxide particles up to 400°C [25-28, 29].

Really, as well known, zirconia is characterized by the presence of both acid and basic sites. However, a net balance between the two kind of sites allows to infer that the surface of pure zirconia mainly behaves as a strong base [30-33]. Indeed, even after sulfation, the surface sites of zirconia result less acidic than those of zeolites [33]. Therefore, the unique properties of zirconia cannot be related to its acidity but they should be interpreted also in terms of basicity.

The basic properties of the studied catalysts were investigated by CO_2 chemisorption/desorption measurements. The data obtained are reported in Table **3** and Fig. (**3**). It is possible to observe that all bulk oxides, MgO, MnO_2 and ZrO_2, show a CO_2 desorption profile spanned in the range 25-350°C revealing the presence of surface basic sites with a broad strength distribution. In particular, MgO sample is

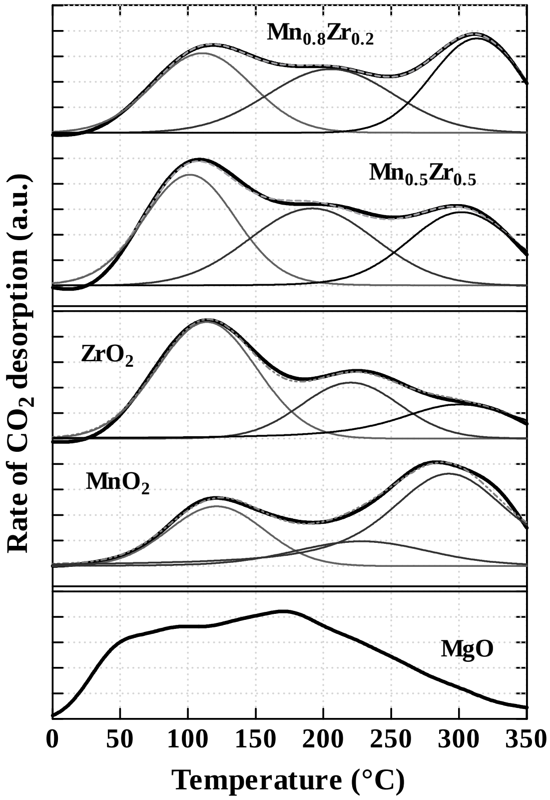

Fig. (3). CO_2 desorption profiles and deconvolution analysis in the range 0-350°C of the "bulk" oxides and $MnZrO_x$ samples.

characterized by the highest specific basicity (363 $\mu mol_{CO2}\cdot g_{cat}^{-1}$), but MnO_2 results to possess the highest basicity referred to the total surface area (2.9 $\mu mol_{CO2}\cdot m^{-2}$). Concerning ZrO_2, the three desorption peaks centred at 114, 220 and 300°C account respectively for *weak*, *medium* and *strong* basic sites mostly corresponding to: i) surface OH^- groups; ii) zirconium-oxygen ion pairs and iii) isolated O^{2-} anions [21, 34]. With regard to the two $MnZrO_x$ systems, by increasing the Mn loading, the specific basicity decreases (417 *vs.* 300 $\mu mol_{CO2}\cdot g_{cat}^{-1}$), as previously observed by studying similar $MnCeO_x$ systems [21], but the different surface area exposure determines for both samples an intrinsic basicity close to 2.0 μmol_{CO2} m^{-2}. Moreover, it is interesting to underline that, by increasing the calcination temperature, the intrinsic basicity increases too: the $Mn_{0.8}Zr_{0.2}$ sample calcined at 600°C exhibits a CO_2 desorption value of 6.9 μmol_{CO2} m^{-2}, with a population of basic sites per unit of surface about two-fold higher than that of the sample calcined at 300 or 400°C, in agreement with the findings reported in literature [35].

In the attempt to discriminate the contribution of basic sites of different strength, a preliminary investigation was performed by a deconvolution analysis of all chemisorption profiles. By these processed data, it was observed that a linear combination of three Gaussian peaks well describes all the experimental curves, providing a very accurate fitting (r^2>0.99) (Fig. **3**). By considering $Mn_{0.5}Zr_{0.5}$ and $Mn_{0.8}Zr_{0.2}$ respectively, the maxima temperature (T_M) slightly shifted towards higher temperatures for each peak; at the same time, the population of medium and strong basic sites (MSBS) per unit of surface area increases with the loading of manganese (Table **3**):

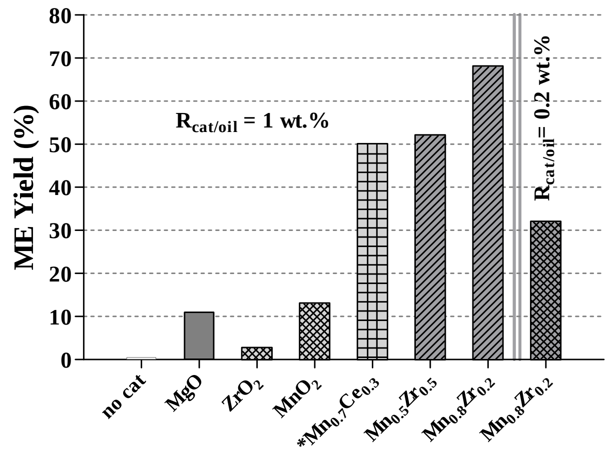

Fig. (4). ME yield (%) on Mn-based systems: sunflower oil weight, 80 g; $R_{met/oil}$, 12 mol/mol; $R_{cat/oil}$, 1 wt.%; T_R, 140°C; reaction time, 1 h (*Ref. [21]).

ZrO_2 (50%) < $Mn_{0.5}Zr_{0.5}$ (63%) < $Mn_{0.8}Zr_{0.2}$ (68%) < MnO_2 (76 %).

Moreover, the sample calcined at high temperature ($Mn_{0.8}Zr_{0.2\_600}$) is characterized by a different distribution of basic sites mainly composed by a prevailing contribution of sites with T_M=130°C and a low population of MSBS (40 %). However, by considering the low surface area of such a system (61 m^2 g^{-1}), the density of strong basic sites per unit of surface area results very high, 1.79 μmol_{CO2} m^{-2}.

The catalytic behaviour of the prepared catalysts was evaluated in the transesterification reaction at 140°C, far away from the equilibrium condition, using a methanol to sunflower oil molar ratio of 12 and a weight catalyst/oil ratio ($R_{cat/oil}$) of 0.2-1. The results obtained are shown in Fig. (**4**). For comparison, the catalytic performance of a structured $MnCeO_x$ system previously investigated [21] is also shown. In absence of catalyst, the reaction does not take place (oil conversion < 1%), while using MgO and MnO_2 "bare" oxides a similar ME yield of 11-13 % was obtained: this result confirmed the catalytic peculiarity of manganese oxide in promoting the transesterification reaction. Low oil conversion has been obtained using zirconia, even if it is characterized by a specific basicity comparable with that of other oxide samples. The poor performance of ZrO_2 could be explainable by considering the microporous structure characterizing this system (APD=28 Å) which makes active sites inaccessible to the sterically hindered TGs molecules.

With regard to the $MnZrO_x$ systems, the $Mn_{0.5}Zr_{0.5}$ sample exhibits a very interesting behaviour, allowing to obtain a ME yield of 52% at 140°C after 1 h of reaction. Such a catalytic performance appears even more interesting if compared with that of previously investigated $MnCeO_x$ system [21]. Indeed, the fact that the $Mn_{0.5}Zr_{0.5}$ sample exhibits a ME yield similar to that of $Mn_{0.7}Ce_{0.3}$ sample (ca. 50%) can be taken as a proof that, on novel $MnZrO_x$ system, a lower Mn loading is required for the obtainment of high ME yield.

Besides, by using the $Mn_{0.8}Zr_{0.2}$ sample, characterized by a higher Mn/Zr atomic ratio (4.0), a ME yield of 68% was attained. This corresponds to a theoretical yield of glycerine of about 4% with a GC purity >98%. Moreover, by using a

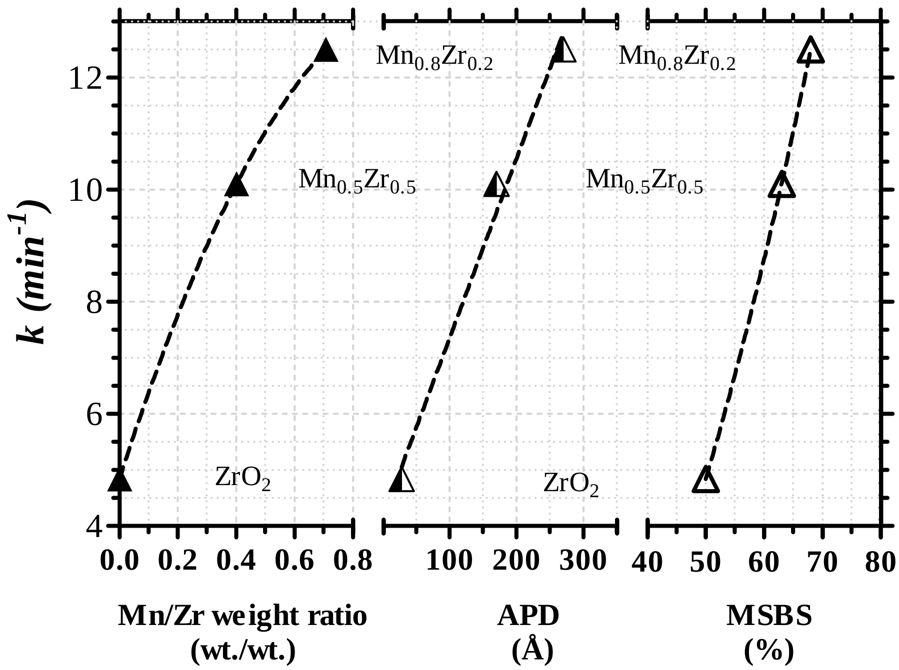

Fig. (5). Correlation among textural and surface properties with catalytic data.

Table 4. Evaluation of Catalyst Stability: Influence of K Loss on Catalyst Performance

Catalyst	K loading[a] (wt.%)	ME Yield* (%)
$Mn_{0.5}Zr_{0.5}$	4.03	83
$Mn_{0.5}Zr_{0.5}$_used 2° run	0.30	42
$Mn_{0.5}Zr_{0.5}$_used 3° run	0.25	40

[a]X-ray Fluorescence.
*$R_{cat/oil}$, 1 wt.%; $R_{met/oil}$, 12 mol/mol; T_R, 140°C; reaction time, 5h.

$R_{cat/oil}$ of 0.2 wt.%, that is at least 5-15 times lower than that normally used in the current literature [9-16], a significant ME yield was still obtained (≈ 32%), thus emphasizing the remarkable activity of $MnZrO_x$ catalysts in the transesterification reaction.

In order to obtain reliable data, not affected by diffusional phenomena, catalytic tests under kinetic regime (oil conversion <10%) were carried out. In the attempt to identify the correlation among textural and surface properties with catalytic data, the values of kinetic constant have been plotted as a function of Mn/Zr weight ratio, average pore diameter (APD) and medium and strong basic sites (MSBS) calculated per unit of surface area (see Fig. **5**). The results reveal that the rate constant (k) increases with the manganese loading, thus confirming the role of Mn as active catalytic species. On the other hand, the kinetic constant values linearly increase with the concentration of medium and strong basic sites and at the same time with the average pore diameter too. These correlations underline that both surface and structural properties synergistically concur to influence the catalytic behaviour, in particular the strength of basic sites being fundamental for the activation of reactant molecules and the accessibility of active sites being a key factor due to the large molecules involved in the reaction [21].

Moreover, in order to take into account all the variables that could affect the catalytic activity of the investigated systems, the attention was also addressed to the presence of K which incorporates into the catalyst structure during the precipitation step. As reported in Table **1**, really the $MnZrO_x$ samples contain a significant amount of potassium, 4.8 and 9.7 wt%. Certainly, by considering that the experiments were performed by using a low catalyst/oil ratio (1wt.%), in any case the amount of K that could dissolve in solution during reaction can be considered very low: 0.03 wt.% in case of catalytic testing of $Mn_{0.5}Zr_{0.5}$ and 0.06 wt.% in case of $Mn_{0.8}Zr_{0.2}$. Anyway, this eventuality was checked and "used" catalysts were analyzed by elemental XRF analysis. From the data reported in Table **4**, XRF measurements, further to reveal that Mn loading remain almost constant, also show that the loading of K after the first run drastically decreases from 4.8 up to 0.30 wt.%, in concomitance of a decreasing of ME yield of about 50%. This result clearly puts in evidence that although the presence of K affects the catalyst activity, the "used" $Mn_{0.5}Zr_{0.5}$ catalyst containing a very low loading of K (0.30 wt.%, which corresponds to a K/oil weight ratio of 0.002 wt.%) still continues to maintain a good performance (ME yield of 43%); therefore K affects catalytic activity, but Mn represents the main active species which catalyzes the transesterification reaction. The 3rd run performed with the used $Mn_{0.5}Zr_{0.5}$ sample further confirmed that catalyst maintains its activity, the ME yield slightly decreasing from 42 to 40%.

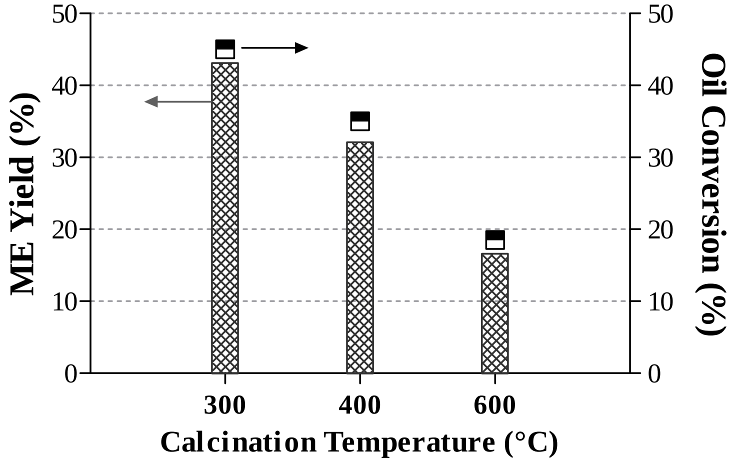

Fig. (6). Influence of the calcination temperature on ME yield (%) and oil conversion: sunflower oil weight, 80 g; $R_{met/oil}$, 12 mol/mol; $R_{cat/oil}$, 1 wt.%; T_R, 140°C; reaction time, 1 h.

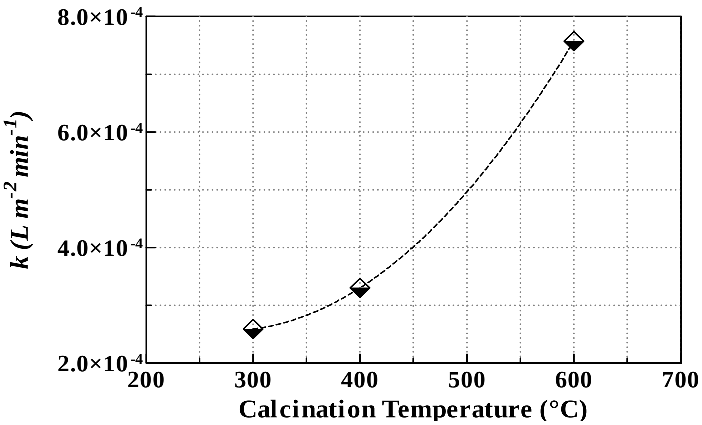

Fig. (7). Effect of the calcination temperature on reaction kinetics evaluated per unit of surface area: sunflower oil weight, 80 g; $R_{met/oil}$, 12 mol/mol; T_R, 140°C; reaction time, 1 h.

However, to exclude the possibility that an important role on overall activity could be exerted also by the presence of K leached from catalyst during the reaction [36], an experiment was carried out in the presence of K in liquid phase. In particular, $Mn_{0.8}Zr_{0.2}$ sample was soaked with pure methanol for 2 h at 140°C; this treatment caused the loss of potassium (from 8.0 to 5.2 wt.%) from the catalyst structure into the alcoholic solution, as confirmed by XRF analysis. Then, the K-containing solution was used as reaction medium for the new experiment. The result obtained was similar to that obtained without catalyst with oil conversion < 1%. Evidently, the low amount of K present in liquid phase does not significantly contribute to alter the catalytic activity of the investigated systems, so pointing out that the (pseudo-)homogeneous catalytic route should be considered not so significant. However, what can appear remarkable is that the leaching of potassium during the transesterification reaction at 140 °C negatively reflects on catalytic activity of $MnZrO_x$ system, since very probably the morphology and structure of catalysts change when K removes from surface.

In conclusion, by considering that K in liquid phase is not active, it can not be inferred other that K plays a structural and electronic role in promoting the activity of manganese, but at moment this should be considered only a hypothesis and further investigations are necessary to demonstrate the role of K in improving the activity of Mn.

As regards the leaching of Mn, AAS analysis of ME and glycerol phases confirmed the presence of trace of manganese, always under 0.012 ppm. Generally, the presence of metals in the biodiesel, is undesirable, as this may cause various problems, including promoting biodiesel degradation, corrosion of engine, operability problems, environmental pollution and subsequent negative effects on human health [37]. However, some organic compound containing manganese have been investigated as additive of the biodiesel fuel since they improve biodiesel properties by reducing the pour point, flash point and viscosity [38].

In the attempt to enhance the interaction of K with catalyst structure, samples were treated at different calcination temperature. As previously discussed, different morphological and surface properties characterize the $Mn_{0.8}Zr_{0.2}$ sample calcined at 300, 400 or 600°C (Tables **2**-**3** and Fig. **2**). As regards the catalytic activity of such samples (see Fig. **6**), after 1 h of reaction, the oil conversion progressively decreases from 45 to 18% when the TC increases. At a first sight, such result demonstrates that calcination at high temperature causes a loss in activity that could be ascribed to the strong shrinkage of the total surface area as reported in Table **2**. However, by reporting the data in terms of kinetic constant per unit of surface area (see Fig. **7**), the best result was observed with the $Mn_{0.8}Zr_{0.2\_600}$ catalyst. By considering the data reported in Table **3**, the catalyst calcined at 600°C possesses a total population of basic sites comparable with catalysts calcined at 300 and 400°C. However, the number of strong basic sites available per unit of surface area is higher when the catalyst is calcined at 600°C (1.79 μmol_{CO2} m^{-2} against 0.66 and 0.88 of the catalysts calcined at 400 and 300 °C respectively). This confirms the relevant role exerted by strong basic sites, although the calcination treatment at 600°C allows to obtain a catalyst structure characterized by a pore size distribution shifted towards the macropores (402 Å). This evidence further stresses the fact that the ideal catalyst for the transesterification reaction should be designed as a system characterized both by high porosity and a large number of strong basic sites.

4. CONCLUSIONS

The MnZrO$_x$ system was found very effective in the methyl esters production by transesterification reaction of sunflower oil with methanol. High methyl esters yields can be obtained at reaction temperature not higher than 140°C by operating at low $R_{cat/oil}$ (1 wt.%) and a methanol/oil molar ratio of 12.

In detail, on the basis of the results obtained, the redox-precipitation method promotes an intimate interaction between manganese and zirconium oxides, allowing the formation of manganese-zirconium oxide domains with high surface area. Moreover, the MnZrO$_x$ system is characterized by a marked basic character, with a broad strength distribution of basic sites. The leaching of potassium into the reaction medium occurs but the fundamental role of Mn as active phase was demonstrated. K was found not active in liquid phase, rather it acts as Mn promoter when incorporated into the catalyst structure. The calcination at high temperature (600°C) negatively reflects on the global catalytic activity although the formation of a macroporous structure is favoured with high strong basic sites accessibility which compensates the loss of activity.

CONFLICT OF INTEREST

The authors confirm that this article content has no conflicts of interest.

ACKNOWLEDGEMENT

Declared none.

REFERENCES

[1] Alsalme, A.; Kozhevnikova, E.F.; Kozhevnikov, I.V. Heteropoly acids as catalysts for liquid-phase esterification and transesterification. *Appl. Catal. A,* **2008**, *349* (1-2), 170-176.

[2] Yan, S.; Salley, S.O.; Simon Ng, K.Y. Simultaneous transesterification and esterification of unrefined or waste oils over ZnO-La2O3 catalysts. *Appl. Catal. A*, **2009**, *353* (2) 203-212.

[3] Yang, R.; Su, M.; Li, M.; Zhang, J.; Hao, X.; Zhang, H. One-pot process combining transesterification and selective hydrogenation for biodiesel production from starting material of high degree of unsaturation. *Bioresour. Technol.*, **2010**, *101* (15), 5903-5909.

[4] Demirbas, A. Progress and recent trends in biofuels. *Prog. Energy Combust. Sci.*, **2007**, *33* (1), 1-18.

[5] Jothiramalingam, R.; Wang, M.K. Review of recent developments in solid acid, base, and enzyme catalysts (heterogeneous) for biodiesel production *via* transesterification. *Ind. Eng. Chem. Res.*, **2009**, *48* (13), 6162-6172.

[6] Lotero, E.; Goodwin Jr, J.G.; Bruce, D.A.; Suwannakarn, K.; Liu, Y.; Lopez, D.E. The catalysis of biodiesel synthesis. *Catalysis*, **2006**, *19*, 41-83.

[7] Kim, H.J.; Kang, B.S.; Kim, M.J.; Park, Y.M.; Kim, D.K.; Lee, J.S.; Lee, K.Y. Transesterification of vegetable oil to biodiesel using heterogeneous base catalyst. *Catal. Today*, **2004**, *93-95*, 315-320.

[8] Bournay, L.; Casanave, D.; Delfort, B.; Hillion, G.; Chodorge, J.A. New heterogeneous process for biodiesel production: A way to improve the quality and the value of the crude glycerin produced by biodiesel plants. *Catal. Today*, **2005**, *106* (1-4), 190-192.

[9] Ebiura, T.; Echizen, T.; Ishikawa, A.; Murai, K.; Baba, T. Selective transesterification of triolein with methanol to methyl oleate and glycerol using alumina loaded with alkali metal salt as a solid-base catalyst. *Appl. Catal. A*, **2005**, *283* (1-2), 111-116.

[10] Kawashima, A.; Matsubara, K.; Honda, K. Development of heterogeneous base catalysts for biodiesel production. *Bioresour. Technol.*, **2008**, *99* (9), 3439-3443.

[11] Cantrell, D.G.; Gillie, L.J.; Lee, A.F.; Wilson, K. Structure-reactivity correlations in MgAl hydrotalcite catalysts for biodiesel synthesis. *Appl.Catal. A*, **2005**, *287* (2), 183-190.

[12] Xie, W.; Peng, H.; Chen, L. Calcined Mg–Al hydrotalcites as solid base catalysts for methanolysis of soybean oil. *J. Mol. Catal. A: Chem.*, **2006**, *246* (1-2), 24-32.

[13] Suppes, G.J.; Bockwinkel, K.; Lucas, S.; Botts, J.B.; Mason, M.H.; Heppert, J.A. Calcium carbonate catalyzed alcoholysis of fats and oils. *J. Am. Oil Chem. Soc.*, **2001**, *78*, 139-145.

[14] Shumaker, J.L.; Crofcheck, C.; Tackett, S.A.; Santillan-Jimenez, E.; Morgan, T.; Ji, Y.; Crocker, M.; Toops, T.J. Biodiesel synthesis using calcined layered double hydroxide catalysts. *Appl. Catal. B*, **2008**, *82* (1-2), 120-130.

[15] Sreeprasanth, P.S.; Srivasta, R.; Srinivas, D.; Ratnasamy, P. Hydrophobic, solid acid catalysts for production of biofuels and lubricants. *Appl. Catal. A*, **2006**, *314* (2), 148-159.

[16] Jitputti, J.; Kitiyanan, B.; Rangsunvigit, P.; Bunyakiat, K.; Attanatho, L.; Jenvanitpanjakul, P. Transesterification of crude palm kernel oil and crude coconut oil by different solid catalysts. *Chem. Eng. J.*, **2006**, *116* (1), 61-66.

[17] Mbaraka, I.K.; Shanks, B.H. Conversion of oils and fats using advanced mesoporous heterogeneous catalysts. *J. Am. Oil Chem. Soc.*, **2006**, *83*, 79-91.

[18] Leclercq, E.; Finiels, A.; Moreau, C. Transesterification of rapeseed oil in the presence of base zeolites and related solid catalyst. *J. Am. Oil Chem. Soc.*, **2001**, *78*, 1161-1165.

[19] Kulkarni, M.G.; Dalai, A.K. Waste Cooking Oil - An Economical Source for Biodiesel: A Review. *Ind. Eng. Chem. Res.*, **2006**, *45* (9), 2901-2913.

[20] Matson, J.V.; Kannan, D.C. Green biodiesel. U.S. Patent 7,563,915, July 21, 2009.

[21] Cannilla, C.; Bonura, G.; Rombi, E.; Arena, F.; Frusteri, F. Highly effective MnCeOx catalysts for biodiesel production by transesterification of vegetable oils with methanol. *Appl. Catal. A*, **2010**, *382* (2), 158-166.

[22] Tanabe, K.; Yamaguchi, T. Acid-base bifunctional catalysis by ZrO2 and its mixed oxides. *Catal. Today*, **1994**, *20* (2), 185-198.

[23] Sunita, G.; Devassy, B.M.; Vinu, A.; Sawant, D.P.; Balasubramanian, V.V.; Halligudi, S.B. Synthesis of biodiesel over zirconia-supported isopoly and heteropoly tungstate catalysts. *Catal. Comm.*, **2008**, *9* (5), 696-702.

[24] Özbay, N.; Oktar, N.; Tapan, N.A. Esterification of free fatty acids in waste cooking oils (WCO): Role of ion-exchange resins. *Fuel*, **2008**, *87* (10-11), 1789-1798.

[25] Arena, F.; Trunfio, G.; Negro, J.; Fazio, B.; Spadaro, L. Basic evidence of the molecular dispersion of MnCeO*x* catalysts synthesized *via* a Novel "Redox-Precipitation" Route. *Chem. Mater.*, **2007**, *19* (9), 2269-2276.

[26] Joint Committee on Powder Diffraction Standards, *ASTM Powder Diffraction Files*; Pennsylvania (PA): Park Lane, Swartmore, **1979**.

[27] European Committee for Standardization. *EN 14103: Fat and oil derivatives – fatty acid methyl esters (FAME) – determination of ester and linolenic acid methyl ester contents*. Brussels (Belgium), **2003**.

[28] Shurvell, H.F. *Spectra-Structure Correlations in the Mid- and Far-infrared*, Wiley & Sons: New York, **2002**.

[29] Arena, F.; Trunfio, G.; Negro, J.; Spadaro, L. Synthesis of highly dispersed MnCeO*x* catalysts *via* a novel "redox-precipitation" route. *Mat. Res. Bull.*, **2008**, *43*, 539-545.

[30] Sauer, J. Acidic sites in heterogeneous catalysis: structure, properties and activity. *J. Mol. Catal.*, **1989**, *54* (3), 312-323.

[31] Aue, D.H.; Bowers, M.T. *Gas-Phase Ion Chemistry*; M.T Bowers, Ed. Academic Press: New York, **1979**; vol. *2*, pp. 1-51.

[32] Brändle, M.; Sauer, J. Acidity differences between inorganic solids induced by their framework structure. A combined quantum mechanics molecular mechanics ab initio study on zeolites. *J. Am. Chem. Soc.*, **1998**, *120* (7), 1556-1570.

[33] Farcasiu, D.; Ghenciu, A.; Qi Li, J. The Mechanism of conversion of saturated hydrocarbons catalyzed by sulfated metal oxides: reaction of adamantane on sulfated zirconia. *J. Catal.*, **1996**, *158* (1), 116-127.

[34] Di Serio, M.; Ledda, M.; Cozzolino, M.; Minutillo, G.; Tesser, R.; Santacesaria, E. Transesterification of soybean oil to biodiesel by using heterogeneous basic catalysts. *Ind. Eng. Chem. Res.*, **2006**, *45* (9), 3009-3014.

[35] Bancquart, S.; Vanhove, C.; Pouilloux, Y.; Barrault, J. Glycerol transesterification with methyl stearate over solid basic catalysts. *Appl. Catal. A*, **2001**, *218* (1-2), 1-11.

[36] Di Serio, M.; Cozzolino, M.; Tesser, R.; Patrono, P.; Pinzari, F.; Bonelli, B.; Santacesaria, E. Vanadyl phosphate catalysts in biodiesel production. *Appl. Catal. A*, **2007**, *320*, 1-7.

[37] Hossain, A.B.M.S.; Mazen, M.A. Effects of catalyst types and concentrations on biodiesel production from waste soybean oil biomass as renewable energy and environmental recycling process. *Aust. J. Crop Sci.*, **2010**, *4* (7), 550-555.

[38] Çaynak, S.; Gürü, M.; Biçer, A.; Keskin, A.; Içingür, Y. Biodiesel production from pomace oil and improvement of its properties with synthetic manganese additive. *Fuel*, **2009**, *88* (3), 534-538.

Received: January 28, 2012 Revised: March 12, 2012 Accepted: April 09, 2012